

## COEXISTING OF CUBIC AND TETRAGONAL PHASES IN PEROVSKITE-TYPE $\text{SrTiO}_3\text{--BiScO}_3$ RELAXOR SYSTEM

E.P. Danshina, O.N. Ivanov, D.A. Kolesnikov

*Joint Research Centre «Diagnostics of Structure and Properties of Nanomaterials»,  
Belgorod State National Research University, Belgorod;  
Danshina@bsu.edu.ru*

*Recommended for Publication by Editorial Member Professor N.Ts. Gatapova*

**Kew words and phrases:** crystal structure; phase coexisting; relaxor ferroelectrics.

**Abstract:** Dielectric anomalies specific for to relaxor ferroelectrics have been found for the  $\text{SrTiO}_3\text{--BiScO}_3$  system. The relaxor properties of this system are rather unexpected because neither  $\text{SrTiO}_3$  nor  $\text{BiScO}_3$  are ferroelectrics. An X-ray diffraction analysis revealed that at room temperature the ceramic  $(1-x)\text{SrTiO}_3\text{--}x\text{BiScO}_3$  samples with  $x = 0.2, 0.3$  and  $0.4$  consist of a mixture of a cubic centrosymmetric  $Pm3m$  phase and a tetragonal polar  $P4mm$  phase. Lattice parameters for these phases increase as  $x$  increases. In addition, it was found by the electron backscattered diffraction method that at room temperature, the fraction of the cubic phase decreases and the fraction of the tetragonal phase increases as the mole fraction of  $\text{BiScO}_3$  increases. Phase coexistence is assumed to be one of the reasons for the relaxor properties of the system under study.

---

Perovskite-type  $\text{SrTiO}_3\text{--BiScO}_3$  system is a new system enabling to study the possibility of ferroelectric state formation in multicomponent systems consisting of non-ferroelectric components.

In this system strontium titanate,  $\text{SrTiO}_3$ , is known to be an incipient ferroelectric lying near the limit of its paraelectric phase stability [1]. Pure  $\text{SrTiO}_3$  retains a nonpolar centrosymmetric crystal on cooling down to the lowest temperature at  $T \rightarrow 0$ . Weak external influences including various impurities substituted for the host ions in crystal structure can destroy a paraelectric state and induce a ferroelectric phase transition in incipient ferroelectrics [2–7].

$\text{BiScO}_3$  is an interesting end member for fabrication of new ceramic solid solutions [8–10]. Despite its utility in solid solutions, there is little knowledge about  $\text{BiScO}_3$  member itself. Although it has been speculated that it may be ferroelectric, no experimental confirmations have been reported [11].

The factors favouring the formation of the ferroelectric state in the  $\text{SrTiO}_3\text{--BiScO}_3$  system consisting of non-ferroelectric end members are as follows:

(i) The crystal symmetries of end members are significantly different. At room temperature  $\text{SrTiO}_3$  has a cubic  $Pm3m$  structure, while  $\text{BiScO}_3$  is a non-polar monoclinic  $C2/c$  compound [12]. So, formation of some intermediate phases with

symmetries other than cubic  $\text{SrTiO}_3$  symmetry and monoclinic  $\text{BiScO}_3$  symmetry can be assumed for  $\text{SrTiO}_3\text{--BiScO}_3$  system. Such intermediate phases including possibly having polar structures are necessary to ensure a significant change in the crystal structure of the system under consideration as the mole fraction of  $\text{BiScO}_3$  increases.

(ii) As it was mentioned above  $\text{SrTiO}_3$  is one of incipient ferroelectrics. Therefore, one can assume that the substitution on the *A*-site by Bi and on the *B*-site by Sc in the  $\text{SrTiO}_3$  structure will destroy a paraelectric state in the  $\text{SrTiO}_3\text{--BiScO}_3$  system.

In fact, it was recently found that the  $\text{SrTiO}_3\text{--BiScO}_3$  system is characterized by dielectric anomalies specific for relaxor ferroelectrics or ferroelectrics with diffuse phase transition [13, 14]. The main features of relaxors are connected with their structural (compositional) inhomogeneity [15–17]. In terms of structural features the relaxor properties can be attributed to coexistence and interaction of polar and non-polar phases in the temperature range of relaxor state existence. Preliminary results have allowed us to conclude that coexistence of polar tetragonal  $P4mm$  phase and non-polar cubic  $Pm3m$  phase can lead to appearance of relaxor properties of the  $\text{SrTiO}_3\text{--BiScO}_3$  system [13–14].

The main purpose of this paper is to characterize further two-phase state in ceramic samples of the  $\text{SrTiO}_3\text{--BiScO}_3$  relaxor system.

Ceramic samples of  $(1-x)\text{SrTiO}_3\text{--}x\text{BiScO}_3$  with  $x = 0.2, 0.3$  and  $0.4$  were synthesized via solid-state processing techniques from powders of  $\text{SrCO}_3$ ,  $\text{TiO}_2$ ,  $\text{Bi}_2\text{O}_3$  and  $\text{Sc}_2\text{O}_3$  taken as starting materials. After preliminary milling and drying, powders were calcined at  $1073\text{ K}$  for  $4\text{ h}$  and at  $1123\text{ K}$  for  $4\text{ h}$  in an air atmosphere.

The calcined powders were then cold isostatically pressed at  $400\text{ MPa}$ . The pressed samples were sintered at  $1623\text{ K}$  for  $5\text{ h}$ . The weight loss during sintering was confirmed to be  $< 1\%$  for all samples. The densities of all samples were higher than  $90\%$  of the value of the theoretical density.

X-ray diffraction (**XRD**) analysis was performed at room temperature for phase composition and crystal structure determination using a Rigaku Ultima IV diffractometer with  $\text{CuK}\alpha$  radiation (a step width of  $0.02^\circ$  and a counting time of  $1\text{ s/step}$ ). A scanning electron microscope, the Quanta 200 3D, was used to apply the electron backscattered diffraction (**EBSD**) method to estimate the distribution of tetragonal and cubic phases in the samples under study (for an accelerating voltage of  $20\text{ kV}$  and a typical current of  $12\text{ nA}$ ). The dielectric permittivity  $\varepsilon$  was measured using a BR2876 LRC-meter at a frequency of  $1\text{ MHz}$ .

Before to characterize the features of two-phase state, let us consider the dielectric properties of the compositions under study.

Figure 1 shows the dielectric permittivity versus temperature for the samples with  $x = 0.2, 0.3$  and  $0.4$ . Broad peaks of  $\varepsilon$  are observed in the  $T$ -dependences for these compositions. It was found that maximum value of dielectric permittivity,  $\varepsilon_m$ , and temperature of the  $\varepsilon(T)$  maximum,  $T_m$ , increase as  $x$  increases.

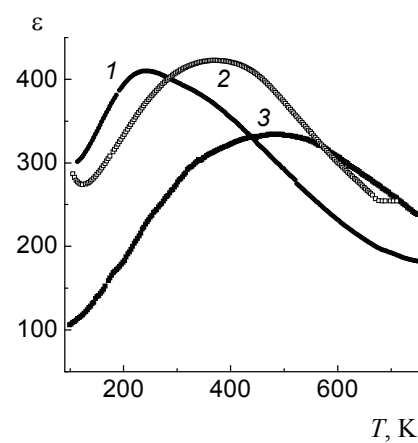


**Fig. 1. Temperature dependences of  $\varepsilon$  for the  $(1-x)\text{SrTiO}_3\text{--}x\text{BiScO}_3$  samples:**  
1 –  $x = 0.2$ ; 2 –  $0.3$ ; 3 –  $0.4$

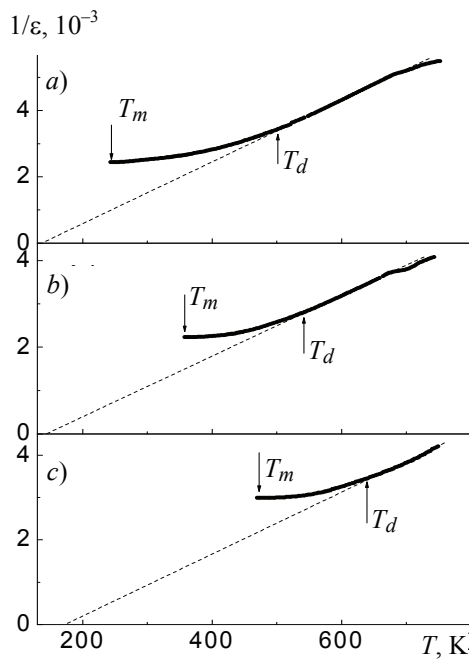


**Fig. 2. Temperature dependences of  $1/\epsilon$  for of  $(1-x)\text{SrTiO}_3-x\text{BiScO}_3$  samples:**  
 $1 - x = 0.2; 2 - 0.3; 3 - 0.4$   
 phase transition [18].

The temperatures  $T_m$  and  $T_d$  extracted from the  $\epsilon(T)$  dependences are listed in Table. According to Table, both temperatures are shifted to the high temperature range as  $x$  increases.

Because the temperature  $T_d$  is higher than room temperature,  $T_R$ , all of the compositions under investigation at  $T_R$  are in the relaxor state in which the polar and nonpolar phases coexist. The characteristics of the crystal lattice for these phases and the phase distribution should be  $x$ -dependent.

XRD analysis was applied to characterize the crystal structure features for sintered  $(1-x)\text{SrTiO}_3-x\text{BiScO}_3$  samples. The XRD patterns taken at  $T_R$  are shown in Fig. 3. The XRD pattern for pure  $\text{SrTiO}_3$  is also presented in this figure. The compositions with  $x = 0.2, 0.3$  and  $0.4$  consist of a mixture of the cubic  $Pm3m$  phase and the tetragonal  $P4mm$  phase, while the composition with  $x = 0$  has cubic  $Pm3m$  symmetry.

### Characteristics of $(1-x)\text{SrTiO}_3-x\text{BiScO}_3$ samples

$x$	$T_m$ , K	$T_d$ , K	Lattice parameter for the cubic phase, $a_c$ , Å	Lattice parameters for the tetragonal phase		Tetragonality, $c_T/a_T$	Tetragonal phase fraction
				$a_T$ , Å	$c_T$ , Å		
0.20	245	505	3.908	3.916	3.923	1.0018	0.25
0.30	358	550	3.931	3.921	3.930	1.0023	0.43
0.40	470	640	3.937	3.932	3.948	1.0041	0.67

For ferroelectrics with a sharp phase transition, the temperature dependence of  $\epsilon$  for the high-temperature part of the  $\epsilon(T)$  peak obeys the Curie-Weiss law

$$\epsilon = \frac{C_{CW}}{T - T_m}, \quad (1)$$

where  $C_{CW}$  is the Curie-Weiss constant and the temperature  $T_m$  is coincident with the Curie temperature. In this case the dependence of  $1/\epsilon$  versus temperature (or the temperature difference  $(T - T_m)$ ) should be linear. Figure 2 shows that experimental  $\epsilon(T)$  curves are linear above some temperature  $T_d$ . Just below  $T_d$  experimental curves start to deviate from the Curie-Weiss behavior.

A broad maximum in the  $\epsilon(T)$  dependence with the characteristic temperature  $T_d$  can be originated from a diffuse phase transition. The temperature  $T_d$ , called the Burns temperature, corresponds to the appearance of the polar phase during the diffuse ferroelectric

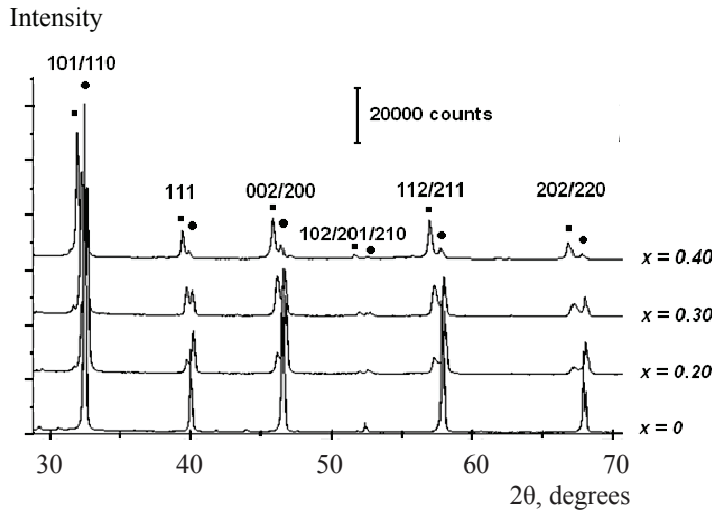


**Fig. 3.** X-ray diffraction patterns of the  $(1-x)\text{SrTiO}_3-x\text{BiScO}_3$  samples:  
◆ –  $\text{Pm}3\text{m}$ ; ■ –  $\text{P}4\text{mm}$

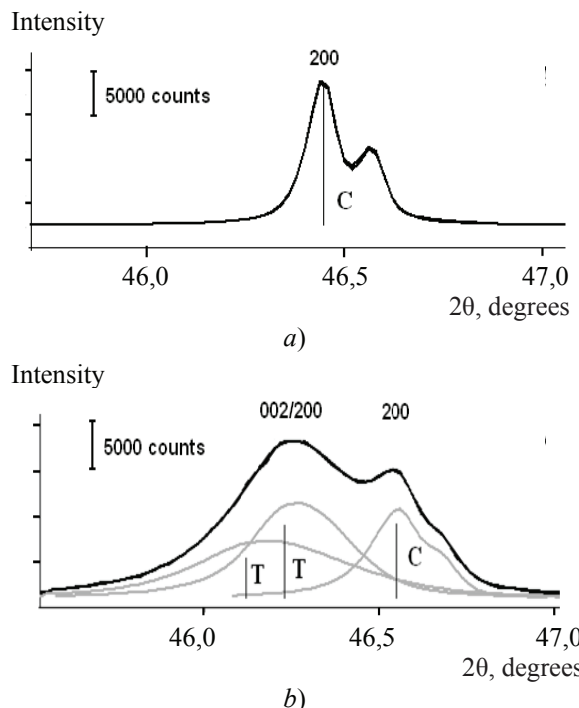


**Fig. 4.** Enlarged part of the diffraction peak in the range  $2\theta = 51.2 - 53.5$  for the sample with  $x = 0$  (a) and  $x = 0.3$  (b):  
C – cubic phase; T – tetragonal phase

The tetragonal  $\text{P}4\text{mm}$  structure is characterized by splitting of the single cubic (200) peak into double diffraction (002)/(200) peaks, as is shown in Fig. 4.

Additional right-side peaks in Fig. 4 are due to the  $\text{CuK}_{\alpha 2}$  radiation. The methods of Savitzky–Golay [19] and Sonneveld–Visser [20] were applied to analyze the XRD patterns. The grey lines in Fig. 4 give the diffraction peaks calculated using this

analysis. The lattice parameters were determined from at least six or four indexed diffraction peaks for the tetragonal ( $a_T$  and  $b_T$ ) and cubic ( $a_C$ ) phases, respectively. The concentration dependencies of the lattice parameters for these phases extracted from the XRD patterns are listed in Table. All lattice parameters in Table increase as  $x$  increases. Such behaviour is predicted when taking into account the difference in radii for pairs of ions at equivalent sites in the perovskite  $\text{ABO}_3$  lattice ( $r(\text{Sr}^{2+}) = 1.12 \text{ \AA}$ ,  $r(\text{Bi}^{3+}) = 1.34 \text{ \AA}$  for the  $A$ -sublattice and  $r(\text{Ti}^{4+}) = 0.745 \text{ \AA}$  and  $r(\text{Sc}^{3+}) = 0.885 \text{ \AA}$  for the  $B$ -sublattice). Because of the significant difference in the ionic radii,  $r(\text{Sr}^{2+})/r(\text{Bi}^{3+}) = 0.836$ , and  $r(\text{Ti}^{4+})/r(\text{Sc}^{3+}) = 0.842$ , the unit cell volume drastically increases as the mole fraction of  $\text{BiScO}_3$  increases. It should also be noted that the tetragonality degree,  $c_T/a_T$ , is small and that it gradually increases as  $x$  increases.

To obtain additional evidence of the coexistence of two phases in the samples of the  $(1-x)\text{SrTiO}_3-x\text{BiScO}_3$  system, the EBSD method was applied (Fig. 5).

Based on the symmetries of the tetragonal and cubic phases determined from XRD analysis, the phase distribution can be mapped by this method. The top images in Figure 5 are EBSD inverse-pole-figure maps for the cubic phase (black domains are the tetragonal phase), and the middle images are EBSD inverse-pole-figure maps for the tetragonal phase (black domains correspond to the cubic phase). The bottom images in Fig. 5 show EBSD phase distribution maps for the samples with  $x = 0.2$ ,  $0.3$  and  $0.4$  taken at room temperature. In this figure, the red colour corresponds to the cubic phase, while the green colour represents the tetragonal phase.

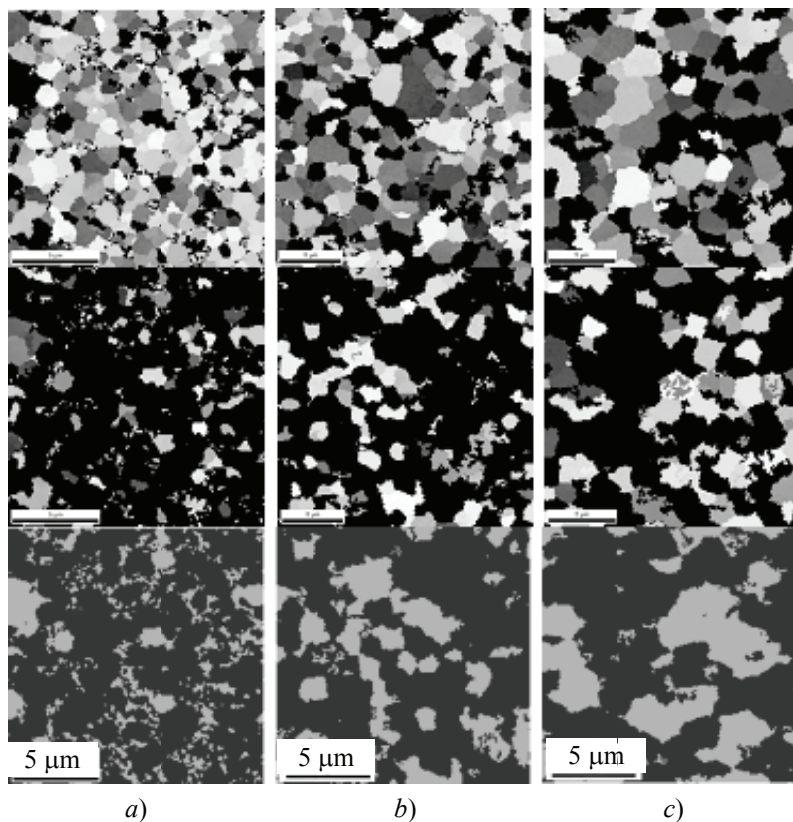


**Fig. 5. EBSD maps for the samples with  $x = 0.2$  (a),  $0.3$  (b) and  $0.40$  (c).**

The top images are EBSD inverse-pole-figure maps for the cubic phase, the middle images are EBSD inverse-pole-figure maps for the tetragonal phase and the bottom images are EBSD phase distribution maps

One can observe that the fraction of the cubic phase decreases and the fraction of the tetragonal phase increases as  $x$  increases. For all compositions, the tetragonal phase is presented by sufficiently large domains whose sizes consistently increased from 2–3  $\mu\text{m}$  for  $x = 0.2$  to 5–7  $\mu\text{m}$  for  $x = 0.4$ . In addition, there are many smaller tetragonal islands with size  $\leq 1 \mu\text{m}$  in the sample with  $x = 0.2$ . Such islands are practically absent for the other compositions.

It is known for relaxors that upon cooling below  $T_d$ , small polar nanodomains appear whose growth and interactions can induce a transition from the relaxor state into a glassy or ordered phase [21]. If the nanodomains grow but do not become large enough, they will ultimately demonstrate a dynamic slowing down of their fluctuations at cooling below  $T_m$ , leading to an isotropic relaxor state with random orientation of the polar domains. If the domains become large enough, the relaxor sample will undergo a cooperative ferroelectric phase transition below  $T_m$ . Thus, a transition from the relaxor state to the ferroelectric state can be assumed for some relaxors.

Figure 5 shows that the polar tetragonal phase is represented by large domains and that the fraction of this phase increase when the Burns temperature shifts to the high-temperature range. This fact can be taken as evidence that for the system under study, the polar nanodomains appearing at  $T_d$  have a tendency towards macroscopic growth and overlapping characteristics for the transition from the relaxor state to the ordered ferroelectric state.

Thus, it is found that the polar  $P4mm$  phase can be formed in the ceramic samples of the  $\text{SrTiO}_3$ – $\text{BiScO}_3$  system consisting of end non-polar members. The tetragonal phase coexists with the cubic centrosymmetric  $Pm3m$  phase. At room temperature, the fraction of the cubic phase decreases and the fraction of the tetragonal phase increases when  $x$  increases. Phase coexistence is assumed to be one of the reasons for the relaxor properties for the system under study.

*This work has been financed by the Ministry of Education and Science of the Russian Federation under Contracts No. 16.552.11.7004 and No. 14.A18.21.1155.*

### References

1. Muller, K.A.  $\text{SrTiO}_3$ : An Intrinsic Quantum Paraelectric Below 4 K / K.A. Muller, H. Burkard // Phys. Rev. B. – 1979. – Vol. 9 – P. 3593–3602.
2. Lemanov, V.V. Improper Ferroelastic  $\text{SrTiO}_3$  and What We Know Today about Its Properties / V.V. Lemanov // Ferroelectrics. – 2002. – Vol. 265. – P. 1–21.
3. Ang, C. Oxygen-Vacancy-Related Low-Frequency Dielectric Relaxation and Electrical Conduction in Bi:  $\text{SrTiO}_3$  / C. Ang, Z. Yu, L.E. Cross // Phys. Rev. B. – 2000. – Vol. 62. – P. 228 – 236.
4. Dielectric Relaxation Modes in Bismuth-Doped  $\text{SrTiO}_3$ : the Relaxor Behavior / C. Ang [et al.] // Phys. Rev. B. – 1999. – Vol. 59. – P. 6670–6674.
5. Dielectric Relaxation in  $\text{SrTiO}_3$ – $\text{SrMg}_{1/3}\text{Nb}_{2/3}\text{O}_3$  and  $\text{SrTiO}_3$ – $\text{SrSc}_{1/3}\text{Ta}_{2/3}\text{O}_3$  Solid Solutions / V.V. Lemanov [et al.] // Appl. Phys. Lett. – 2000. – Vol. 77. – P. 4205–4207.
6. Bi:  $\text{SrTiO}_3$ : a Quantum Ferroelectric and a Relaxor / C. Ang [et al.] // Phys. Rev. B. – 1998. – Vol. 57. – P. 7403–7406.
7. Bednorz, J.G.  $\text{Sr}_{1-x}\text{Ca}_x\text{TiO}_3$ : an XY Quantum Ferroelectric with Transition to Randomness / J.G. Bednorz, K.A. Muller // Phys. Rev. Lett. – 1984. – Vol. 52. – P. 2289–2301.
8. Preparation and Characterization oh High Temperature Perovskite Ferroelectrics in the Solid-Solution  $(1-x)\text{BiScO}_3$ – $x\text{PbTiO}_3$  / R.E. Eitel [et al.] // Jpn. J. Appl. Phys. – 2002. – Vol. 4. – P. 2099–2104.

9. Zhang, S. High Curie Temperature Piezocrystals in the  $\text{BiScO}_3$ – $\text{PbTiO}_3$  Perovskite System / S. Zhang, C.A. Randall, T.R. Shrout // Appl. Phys. Lett. – 2003. – Vol. 83. – P. 3150–3152.
10. Ogihara, H. Weakly Coupled Relaxor Behavior of  $\text{BaTiO}_3$ – $\text{BiScO}_3$  Ceramics / H. Ogihara, C.A. Randall, S. Trolier-McKinstry // J. Am. Ceram. Soc. – 2009. – Vol. 92. – P. 110–118.
11. Growth, Crystal Structure, and Properties of Epitaxial  $\text{BiScO}_3$  thin Films / S. Trolier-McKinstry [et al.] // J. Appl. Phys. – 2008. – Vol. 104. – P. doi 044102-01-07.
12.  $\text{BiScO}_3$ : Centrosymmetric  $\text{BiMnO}_3$ -type Oxide / A.A. Belik [et al.] // J. Am. Chem. Soc. – 2006. – Vol. 128. – P. 706–707.
13. Ferroelectricity in  $\text{SrTiO}_3$ – $\text{BiScO}_3$  System / O. Ivanov [et al.] // Physica Stat. Sol. (b). – 2011. – Vol. 248. – P. 1006 – 1009.
14. Diffuse Phase Transition and Ferroelectric Properties of Ceramic Solid Solution in New  $\text{SrTiO}_3$ – $\text{BiScO}_3$  System / O. Ivanov [et al.] // Advances in Science and Technology. – 2010. – Vol. 67. – P. 59–63.
15. Cross, L.E. Relaxor ferroelectrics / L.E. Cross // Ferroelectrics. – 1994. – Vol. 151. – P. 305–320.
16. Neutron Diffuse Scattering from Polar Nanoregions in the Relaxor  $\text{Pb}(\text{Mg}_{1/3}\text{Nb}_{2/3})\text{O}_3$  / K. Hirota [et al.] // Phys. Rev. B. – 2002. – Vol. 65. – P. 104–105.
17. Gridnev, S.A. Dielectric Relaxation in Disordered Polar Dielectrics / S.A. Gridnev // Ferroelectrics. – 2002. – Vol. 266. – P. 171–209.
18. Bunras, G. Glassy Polarization Behaviour in  $\text{K}_2\text{Sr}_4(\text{NbO}_3)_{10}$ -Type Ferroelectrics / G. Bunras, F.H. Dacol // Phys. Rev. B. – 1984. – Vol. 30. – P. 4012–4013.
19. Savitzky, A. Smoothing and Differentiation of Data by Simplified Least Squares Procedures / A. Savitzky, M.J.E. Golay // Analytical Chemistry. – 1964. – Vol. 36. – P. 1627–1639.
20. Sonneveld, E.J. Automatic Collection of Powder Data from Photographs / E.J. Sonneveld, J.W. Visser // J. Appl. Cryst. – 1975. – Vol. 8. – P. 1–7.
21. Heat Capacity and Thermal Expansion Study of Relaxor-Ferroelectric  $\text{Ba}_{0.92}\text{Ca}_{0.08}\text{Ti}_{0.76}\text{Zr}_{0.24}\text{O}_3$  / M. Gorev [et al.] // J. Phys. Condens. Matter. – 2004. – Vol. 16. – P. 7143–7150.

## Со<sup>существование</sup> кубической и тетрагональной фаз в релаксорной системе $\text{SrTiO}_3$ – $\text{BiScO}_3$ перовскитового типа

**Е.П. Данышина, О.Н. Иванов, Д.А. Колесников**

*Центр коллективного пользования научным оборудованием  
«Диагностика структуры и свойств наноматериалов»,  
ФГАОУ ВПО «Белгородский государственный национальный  
исследовательский университет» (НИУ «БелГУ»), г. Белгород;  
Danshina@bsu.edu.ru*

**Ключевые слова и фразы:** кристаллическая структура; релаксорные сегнетоэлектрики; со<sup>существование</sup> фаз.

**Аннотация:** Диэлектрические аномалии, характерные для релаксорных сегнетоэлектриков, обнаружены при изучении системы  $\text{SrTiO}_3$ – $\text{BiScO}_3$ . Релаксорные свойства этой системы являются достаточно неожиданными, так как ни  $\text{SrTiO}_3$ , ни  $\text{BiScO}_3$  не являются сегнетоэлектриками. Рентгеновский анализ обнаружил, что при комнатной температуре керамические образцы  $(1-x)\text{SrTiO}_3$ – $x\text{BiScO}_3$  с  $x = 0.2, 0.3$  и  $0.4$  состоят из смеси кубической центросимметричной  $Pm3m$  фазы и тетрагональной полярной  $P4mm$  фазы. Параметры решеток этих фаз возрастают

при увеличении  $x$ . Кроме того, с помощью метода дифракции обратно рассеянных электронов, обнаружено, что при комнатной температуре доля кубической фазы уменьшается, а доля тетрагональной фазы возрастает при увеличении мольной доли  $\text{BiScO}_3$ . Предполагается, что существование фаз является одной из причин появления релаксорных свойств исследуемой системы.

---

### Koexistenz der kubischen und tetragonalen Phasen im Relaxorsystem $\text{SrTiO}_3 - \text{BiScO}_3$ des Perowskittypus

**Zusammenfassung:** Die dielektrischen Anomalien, die für die Relaxorferroelektriken charakteristisch sind, wurden bei dem Erlernen des Systems  $\text{SrTiO}_3 - \text{BiScO}_3$  nachgewiesen. Die Relaxoreigenschaften dieses Systems sind genug unerwartet, weil weder  $\text{SrTiO}_3$  noch  $\text{BiScO}_3$  keine Ferroelektriken sind. Die Röntgenanalyse hat gezeigt, dass bei der Zimmertemperatur die keramischen Muster  $(1-x)\text{SrTiO}_3 - x\text{BiScO}_3$  c  $x = 0.2, 0.3$  und  $0.4$  aus dem Gemisch der kubischen zentrosymmetrischen  $Pm3m$  Phase und der tetragonalen polaren  $P4mm$  Phase bestehen. Die Parameter der Gitter dieser Phasen steigern bei der Vergrösserung von  $x$ . Ausserdem wurde es mit Hilfe der Methode der Diffraction der indirect diffusen Elektronen entdeckt, dass bei der Zimmertemperatur der Anteil der kubischen Phase kleiner wird, und der Anteil der tetragonalen Phase bei der Vergrösserung des Molanteiles  $\text{BiScO}_3$  grösser wird. Es wird angenommen, dass die Koexistenz der Phasen einer der Gründe des Erscheinens der Relaxoreigenschaften des untersuchenden Systems ist.

---

### Coexistence des phases cubique et tétragonale dans un système de relaxion $\text{SrTiO}_3 - \text{BiScO}_3$ du groupe de la pérokvskite

**Résumé:** Les anomalies diélectriques typique pour les ferroélectriques de relaxion sont révélées lors de l'étude du système  $\text{SrTiO}_3 - \text{BiScO}_3$ . Les propriétés de relaxion de ce système sont assez inattendues puisque ni  $\text{SrTiO}_3$ , ni  $\text{BiScO}_3$  ne sont pas ferroélectriques. L'analyse radiologique a montré que lors de la température de chambre les échantillons céramiques  $(1-x)\text{SrTiO}_3 - x\text{BiScO}_3$  c  $x = 0.2, 0.3$  et  $0.4$  se composent du mélange centrosymétrique cubique de la phase  $Pm3m$  et de la phase tétragonale polaire  $Pm4m$ . Les paramètres des réseaux de ces phases augmentent lors de la croissance  $x$ . Outre cela à l'aide de la méthode de la diffraction des électrons dispersés inversement il est révélé que lors de la température de chambre la part de la phase cubique diminue et celle de la phase tétragonale augmente avec l'augmentation de la part modulaire  $\text{BiScO}_3$ . Est supposé que la coexistence des phases est une des raisons de l'apparition des propriétés de relaxion du système étudié.

---

**Авторы:** *Даншина Елена Павловна* – кандидат физико-математических наук, научный сотрудник Центра коллективного пользования «Диагностика структуры и свойств наноматериалов»; *Иванов Олег Николаевич* – доктор физико-математических наук, директор Центра коллективного пользования «Диагностика структуры и свойств наноматериалов»; *Колесников Дмитрий Александрович* – заведующий лабораторией микроскопии и рентгеноструктурного анализа Центра коллективного пользования «Диагностика структуры и свойств наноматериалов», ФГАОУ ВПО «Белгородский государственный национальный исследовательский университет» (НИУ «БелГУ»), г. Белгород.

**Рецензент:** *Красильников Владимир Владимирович* – доктор физико-математических наук, профессор кафедры «Материаловедение и нанотехнологии», ФГАОУ ВПО «Белгородский государственный национальный исследовательский университет» (НИУ «БелГУ»), г. Белгород.